Bioorganic & Medicinal Chemistry Letters 23 (2013) 2384–2390

Contents lists available at SciVerse ScienceDirect

Bioorganic & Medicinal Chemistry Letters

journal homepage: www.elsevier.com/locate/bmcl

Optimization of allosteric MEK inhibitors. Part 1: Venturing into underexplored SAR territories

Ingo V. Hartung [a,*], Marion Hitchcock [a], Florian Pühler [b], Roland Neuhaus [c], Arne Scholz [b], Stefanie Hammer [b], Kirstin Petersen [b], Gerhard Siemeister [b], Dominic Brittain [a,†], Roman C. Hillig [d]

[a] Medicinal Chemistry, Bayer HealthCare AG, 13353 Berlin, Germany
[b] Therapeutic Research Group Oncology, Bayer HealthCare AG, 13353 Berlin, Germany
[c] Research Pharmacokinetics, Bayer HealthCare AG, 13353 Berlin, Germany
[d] Structural Biology, Bayer HealthCare AG, 13353 Berlin, Germany

ARTICLE INFO

Article history:
Received 11 December 2012
Revised 1 February 2013
Accepted 7 February 2013
Available online 14 February 2013

Keywords:
Allosteric MEK inhibitor
Oncology
Structure-based drug design
Blood–brain barrier

ABSTRACT

Using PD325901 as a starting point for identifying novel allosteric MEK inhibitors with high cell potency and long-lasting target inhibition in vivo, truncation of its hydroxamic ester headgroup was combined with incorporation of alkyl and aryl ethers at the neighboring ring position. Whereas alkoxy side chains did not yield sufficient levels of cell potency, specifically substituted aryloxy groups allowed for high enzymatic and cellular potencies. Sulfamide **28** was identified as a highly potent MEK inhibitor with nanomolar cell potency against B-RAF (V600E) as well as Ras-mutated cell lines, high metabolic stability and resulting long half-lives. It was efficacious against B-RAF as well as K-Ras driven xenograft models and showed—despite being orally bioavailable and not a *P*-glycoprotein substrate—much lower brain/plasma exposure ratios than PD325901.

Co-targeting multiple nodes within one signaling axis (vertical combinations) or co-targeting parallel (possibly interconnected) signaling pathways (horizontal combinations) is becoming more and more the mainstay for clinical research on improving antitumor efficacy and on addressing acquired resistance to highly specific ('targeted') cancer therapeutics. The Ras–Raf–MEK–ERK pathway is one of the most often deregulated pathways in human cancers, with mutated oncogenic forms of Ras having being identified in up to 30% of human cancers and B-Raf mutations being omnipresent in malignant melanomas.[1] Inhibitors of the key signaling node within this pathway, the mitogen activated protein (MAP) kinase kinases MEK1/2 have been shown to be prime experimental combination partners for other targeted cancer therapeutics such as inhibitors of the PI3K-Akt-mTOR pathway (horizontal combination) or inhibitors of Raf or ERK (vertical combination).[2]

Based on pioneering work by researchers at Pfizer, inhibition of MEK1/2 by highly selective allosteric inhibitors has been pursued by many pharmaceutical companies.[3,4] However, the first generation of advanced clinical MEK1/2 inhibitors, namely PD325901 and AZD6244, did not yield convincing clinical efficacy. In addition, PD325901 was burdened by ocular toxicity and likely CNS-mediated adverse effects leading to its discontinuation.[5] CNS-mediated adverse effects have not been reported for AZD6244.[6] Taking these clinical findings into account, a new generation of allosteric MEK inhibitors would have to maintain the exquisite target selectivity of its predecessors while improving their PK profile, more specifically by reducing brain penetration and at the same time securing continuous target inhibition upon once-daily oral dosing.[7]

Inhibitors from Pfizer's PD series of 2-anilino-benzoic acids are binding to an allosteric site not overlapping with the ATP binding site which is more commonly targeted by kinase inhibitors. Based on crystallization of MEK1/2 with a close analog of PD325901 key enzyme–ligand interactions have been deduced[8] and later-on confirmed by SAR findings (highlighted in Fig. 1).[9] Subsequent medicinal chemistry efforts were largely focused on retaining, mimicking or strengthening these interactions. However, up to 2008 literally no efforts had been invested into introducing functionalized substituents to the 6-position of the benzoic acid core.[10] To the contrary, it had been stated that substituents at the C6 position would be detrimental for target potency.[11]

Taking the history of kinase inhibitor design into account, especially Gleevec with its DFG-out binding mode, one can hypothesize that growing kinase inhibitors into previously unexplored binding regions may lead to induced fit binding pocket adaptions which may result in strikingly different pharmacological profiles. As the hydroxamic acid linkage was one known metabolic liability of PD-like MEK inhibitors, truncating this functionality while at the same time introducing a functionalized alkoxy ether side chain at

* Corresponding author. Address: Bayer HealthCare AG, Global Drug Discovery, Müllerstraße 178, 13353 Berlin, Germany.
E-mail address: ingo.hartung@bayer.com (I.V. Hartung).
† Pharma Strategy, Novartis Pharma AG, Bottmingen CH-4103, Switzerland.

0960-894X/$ - see front matter © 2013 Elsevier Ltd. All rights reserved.
http://dx.doi.org/10.1016/j.bmcl.2013.02.028

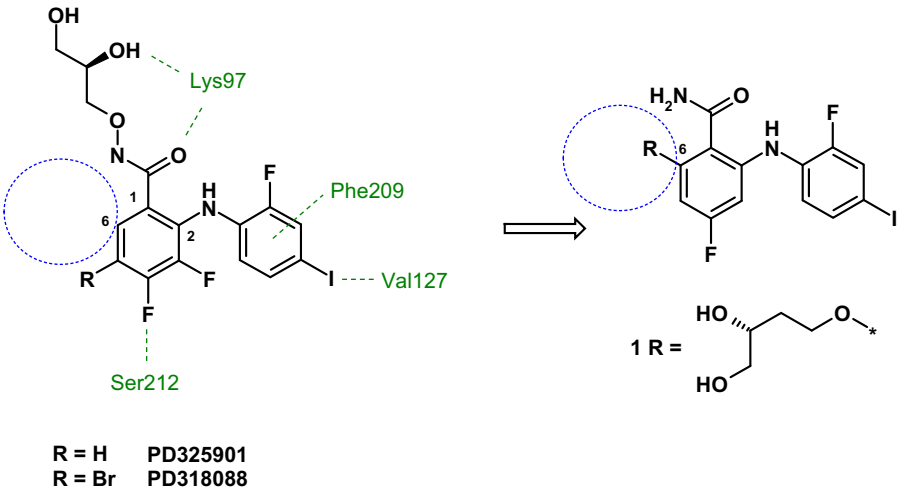

Figure 1. Key ligand–protein interactions for PD325901 (highlighted in green)—Rationale for introduction of side chains at C6 position.

the C6 position appeared to be a promising starting point for identifying novel allosteric MEK inhibitors.[12]

Encouragingly, from a focused number of analogs initially synthesized, hydroxyl-alkoxy ether **1** proved this rationale to be a viable path forward. In this Letter we describe the characterization of this new allosteric C6-*alkoxy* benzoic amide MEK inhibitor and our subsequent optimization program leading to C6-*aryloxy* derivatives with high enzymatic and cellular potency, exceptionally long half-lives and convincing efficacy at low oral doses in mice xenograft models driven by either B-Raf or K-Ras mutations.

Newly synthesized compounds were profiled in an enzymatic COT-MEK-ERK1 cascade assay and optionally in cell proliferation assays employing A375 cells, harboring a B-Raf (V600E) mutation, and HCT116 cells, harboring a K-Ras G13D mutation.[13,14] In line with previous publications, A375 cells were found to be significantly more sensitive to MEK inhibition than HCT116 cells.[15]

Our lead MEK inhibitor **1** was found to be a moderately potent MEK inhibitor (Table 1). An enzymatic IC_{50} of 63 nM compared well to AZD6244 (80 nM), whereas both compounds were significantly less potent than PD325901 (7 nM) in this assay. In cell assays, **1** showed inhibition of A375 proliferation with a sub-μM IC_{50}, but μM concentrations were required to effect inhibition of proliferation of the K-Ras mutated cell line HCT116.

Our lead **1** showed low-to-moderate clearance in rats, a half-life of 2.4 h and 70% bioavailability (Table 4). Of concern to us, **1** significantly crossed the blood–brain barrier in mice, even exceeding the brain/plasma exposure ratio obtained with PD325901 under similar conditions. Hence, though being a valuable starting point, the profile of **1** required significant further optimization with the need to increase enzymatic and cell potency and to reduce brain penetration.

A co-crystal structure of **1** with MEK1 was solved in order to guide our potency optimization efforts (Protein Data Bank accession code 4ark). As can be deduced from Figure 2, almost all the canonical core interactions with the MEK enzyme were preserved: Compound **1** binds in a deep hydrophobic pocket and forms numerous van der Waals contacts with Met143, Leu118, Ile141 and a T stacking interaction with Phe209. However, Lys97 which binds to the hydroxyl and carbonyl group of the hydroxamic ester in PD-type compounds is not engaged in any interactions with compound **1**. These missing interactions may explain the drop in potency between **1** and PD325901 (in addition to an unknown impact of the second fluorine atom at the PD325901 core). At the same time, the newly introduced C6 side chain did not show productive hydrogen bonding interaction aside from a tentatively assigned interaction between the terminal hydroxyl group with the side chain of Asp190 (3.5 Å).

Our initial goal for the first round of SAR work was to convert the C6 ether side chain from a bystander group as in **1** (with a potentially beneficial impact on physicochemical and PK properties) to a group driving target potency. Therefore refraining from re-introducing the hydroxamic ester moiety, we focused instead on optimizing the C6 ether side chain. Selected and most instructive analogs from this endeavor are compiled in Table 1. Simplifying the C6 ether side chain to a methoxy group (**2**) further reduced cell potency, whereas inverting the stereocenter (**3**) or moving it to a different position (**4**) was of only minor impact. Increasing lipophilicity by methylation gave rise to tertiary alcohol **6** with an IC_{50} of 40 nM in the A375 proliferation assay. However, in the less sensitive K-Ras driven HCT116 proliferation assay still μM concentrations were required. Replacing the terminal hydroxyl group by various amines (e.g., $–NH_2$, –NH-Et, morpholine, N-Me-piperazine) was accepted on the enzymatic level but less favorable with respect to cellular potency (data not shown). Introduction of small heterocycles as capping moieties (e.g., pyrazole **7** and imidazole **8**) similarly improved enzymatic potency but did not translate well into cell potency.

Imidazole **8**—with in vitro and cell potency comparable to AZD6244 but inferior to PD325901—showed an interesting PK profile (Table 4). Clearance was low in rats, and volume of distribution high (reflecting the basicity of the imidazole ring) resulting in a long terminal half-life. Bioavailability in rats was low (29%), significantly below what would be expected based on the observed low in vivo clearance. Since we measured significant efflux in the Caco2 permeability assay (~10-fold efflux for **8** compared to ~threefold influx for **1**), absorption into the circulation is likely limited by active efflux. Compound **8** was shown to be a *P*-glycoprotein (Pgp) substrate in vitro. Accordingly, brain penetration of **8** in mice was also significantly attenuated compared to **1**. In conclusion, by replacing the terminal hydroxyl group in **1** by an imidazole group our goal of significantly reducing brain exposure was reached. However, we felt the potency of imidazole **8** to be insufficient and the overall PK profile to be unfavorable for an oral drug.

Reducing the degree of side-chain flexibility in order to improve potency was subsequently pursued by introducing various heterocycloalkyl groups into the C6 side-chain. One exemplary series (out of a structurally diverse set of cyclic side-chains pursued) is shown in Table 2. Unsubstituted prolinol (**9**) gave similar enzymatic and

Table 1
SAR of C6-alkoxy substituents (according to Fig. 1)

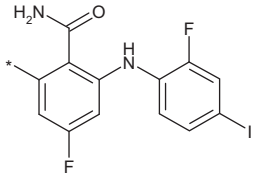

Compound	Side chain	In vitro IC_{50}[a] (nM)		
		MEK1[b]	A375 (B-Raf)	HCT116 (K-Ras)
PD325901		7	13	194
AZD6244		80	31	3100
1	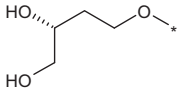	63	148	3400
2		74	354	–
3	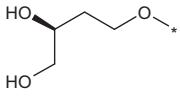	96	240	–
4	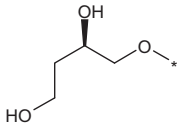	63	350	–
5	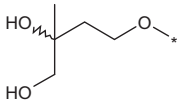	69	240	–
6	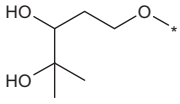	43	40	2450
7	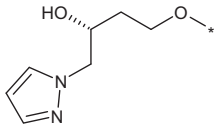	13	151	2070
8	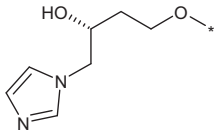	16	98	1250

[a] See text and footnote 13 for assay details.
[b] Lower detection limit of this assay: IC_{50} of ~5–15 nM.

cell potency as our initial side-chain lead **1**. Capping of the side-chain nitrogen did not improve but, to the contrary, in most cases deteriorated potency with the exception of sulfamide **13**.

Having so far not been able to reach sub-μM IC_{50} values in the HCT116 proliferation assay we switched our focus to even less flexible (hetero)-aromatic C6 side-chains (Table 3). Researchers from Japan Tobacco had described their MEK inhibitor JTP-70902 in late 2007 which featured an additional aromatic side-chain (albeit in combination with a significantly different scaffold and a less flexible anchor point; see Figure 3).[16] Interestingly, JTP-70902 resulted from a screen searching for inducers of $p15^{INK4b}$, a downstream effector of the Ras–Raf–MEK–ERK pathway. JTP-70902 is thereby the only allosteric MEK inhibitor not resulting from a structure-based program employing PD-like inhibitors as starting point.

Phenoxy-substituted analog **14** was found to be less potent than our initial lead **1**, whereas a meta-pyridoxy side-chain restored potency to the previously reached level. Introducing a meta-acetamido phenyl side-chain did not lead to the needed potency boost. By systematically assessing substituents on the phenoxy side-chain (exemplary analogs **18**–**21**) several inhibitors with low nanomolar enzymatic and A375 cell potency were identified, but the μM threshold in the HCT116 assay was still not conquered. A breakthrough was accomplished with the striking finding that—despite the methyl sulfonamide analog **22** being not more potent than comparable amide analogs—its higher homolog **23** did show a sub-μM IC_{50} in the HCT116 proliferation assay. Surrounding SAR exploration gave rise to sulfamide **25** which was our most potent analog so far (IC_{50} of 155 nM in the HCT116 proliferation assay) and was therefore profiled in more detail.

Sulfamide **25** showed a moderate blood clearance in rats of 2.1 L/h/kg (1 mg/kg iv dose) with a half-life of 2.2 h and a moderate bioavailability of 55%. Compound **25** was found to be highly efficacious in vivo in a LOX carcinoma mice model employing doses of 1 and 2.5 mg/kg po once-daily (data not shown). In incubations with liver microsomes and hepatocytes, demethylation of the sulfamide moiety was identified as the only metabolic pathway of **25**.

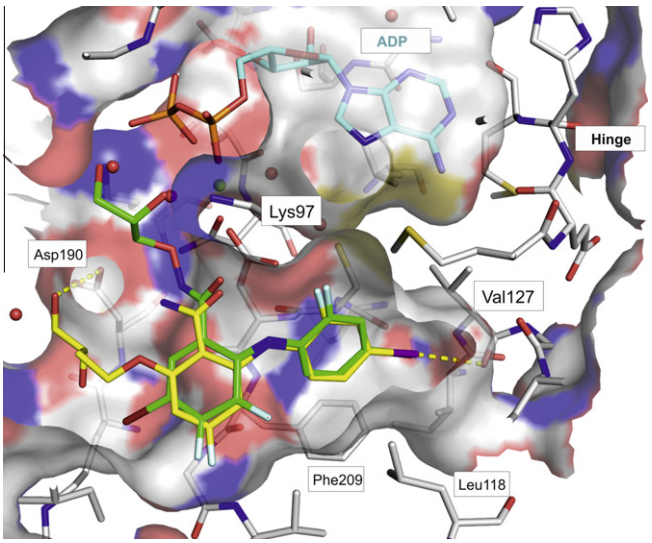

Figure 2. Co-crystal-structure of compound **1** (carbon atoms in yellow) and ADP (cyan) bound to MEK1. For comparison, MEK1 in complex with PD318088 (PDB 1s9j) was superimposed (ligand carbon atoms in green). Figure generated using the Pymol software.

Table 2
SAR of prolinol-containing C6-ether side-chains

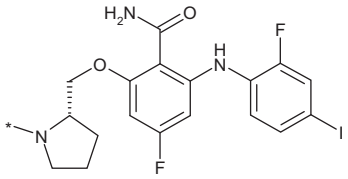

Compound	Side chain	In vitro IC_{50} (nM)		
		MEK1	A375 (B-Raf)	HCT116 (K-Ras)
9		26	124	3030
10		182	973	–
11		96	323	–
12	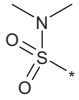	1000	1120	–
13		73	172	3040

Inspired by this metabolic profiling result and being aware that metabolites in certain cases possess superior PK and physicochemical properties than their parent compounds, we synthesized the mono-methylated sulfamide **27** and its unsubstituted congener **28**. The synthesis of sulfamide **28** is summarized in Scheme 1.

Sulfamide **28** is easily accessible in only three steps from 2,4,6-trifluorobenzamide by base-mediated (amide directed) introduction of both *ortho* substituents. It is noteworthy that the C6-meta-aminophenoxy side-chain was introduced without necessitating an amino protection group thereby allowing for direct introduction of the sulfamide capping group in the subsequent and final step. Beneficially, this synthetic route is also easily applicable for screening diverse capping groups.

Analogous synthetic routes were used for all derivatives containing aromatic ether side chains. In the earlier part of the project—especially for the synthesis of compounds with alkyl ether side chains (Table 1)—2,4,6-trifluorobenzonitrile was used as starting material necessitating an additional step for a final H_2O_2-promoted nitrile-to-amide transformation. In contrast to 2,4,6-trifluorobenzamide, base-promoted S_NAr to 2,4,6-tri-fluorobenzonitrile were less regioselective and required tedious separation of *ortho*- and *para*-regioisomers. Hydroxyl groups in alkyl side chains were suitably protected, for example as an acetonide in case of vicinal diols.

Gratifyingly, demethylated analogs **27** and **28** were found to be at least as potent as the dimethylated parent compound **25**. The unsubstituted sulfamide **28** inhibited A375 proliferation with a low nanomolar IC_{50} and was as potent as PD325901 in the HCT116 proliferation assay. Sulfamide **28** was found to be up to 10-fold more potent than AZD6244 in the latter assay as well as in other proliferation assays with non-B-Raf driven cell lines. For example, compound **28** inhibited proliferation of A549 cells with an IC_{50} value of 132 nM (PD325901 166 nM, AZD6244 1750 nM), LOVO cells with an IC_{50} value of 175 nM (PD325901 128 nM, AZD6244 2830 nM) and MIA PaCa-2 cells with an IC_{50} value of 23 nM (PD325901 17 nM, AZD6244 142 nM), respectively.

MEK inhibitor **28** showed low clearance in all investigated species (rat, mouse, dog; see Table 4 for rat data) with long half-lives (32 h in rat, 34 h in mice and 110 h in dogs) and moderate-to-high bioavailabilities. In summary, metabolism-inspired removal of two methyl groups—a strategy which may be coined *pre-metabolization*—improved metabolic stability while target potency was retained. Although not a focus of our optimization strategy at that time, switching to the unsubstituted sulfamide motif also increased the lipophilicity efficiency (decrease of *c*log*P* by 0.8 units).

This very promising in vitro pharmacological and in vivo PK profile translated well into high in vivo efficacy in various xenograft models. For example, a daily dose of 1 mg/kg po was sufficient for complete tumor growth inhibition in an A549 (K-Ras mutated NSCLC) xenograft study in nude mice (Fig. 4). 1 mg/kg of sulfamide **28** (dosed once-daily) was statistically significantly more efficacious than 3 mg/kg PD325901 (once-daily). Due to its long half-life, intermittent dosing schemes (for example 1 mg/kg dosed every second day) were as efficacious in the A549 xenograft setting as daily dosing schemes.

Most notably, sulfamide **28** showed an exceptionally low brain/plasma exposure ratio after iv dosing to mice (Table 4). Low brain penetration potential was confirmed by comparing pERK inhibition by Western blotting of A549 tumor tissue with brain lysates at the highly efficacious dose of 2 mg/kg po (data not shown). Whereas ERK phosphorylation in tumor tissue was almost completely blocked 6 h after dosing, no change in pERK1/2 was observed in brain lysates.

Having constantly profiled analogs from our series for its brain penetration behavior in mice, we tried to rationalize our findings by correlating brain/plasma exposure ratios qualitatively to TPSA values (as a measure for polarity-driven permeability limitations) and Pgp recognition (as one well known mechanism for preventing brain penetration by active efflux).[17] We did not find any hint for Pgp-mediated efflux for sulfamide **28** or for close analogs with similarly limited brain/plasma exposure ratios. For example, sulfamide **28** retained its high pERK inhibitory potency in the Pgp-expressing cancer cell line HeLa-MaTu-ADR whereas AZD6244 experienced a dramatic decrease of pERK inhibitory potency in this cell line. Of note, we found that analogs from our series with a TPSA of 130–140 $Å^2$ possess low brain penetration potential in mice while retaining sufficient bioavailability after oral dosing.

It is noteworthy that crystals of MEK1 incubated with C6-*aryl*oxy-substituted compounds could be grown but never diffracted

Table 3
SAR of C6-aryloxy substituents

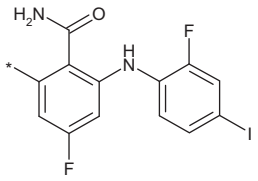

Compound	Side chain	In vitro IC_{50} (nM)		
		MEK1	A375 (B-Raf)	HCT116 (K-Ras)
14	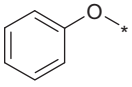	99	408	–
15	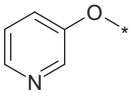	76	141	4180
16	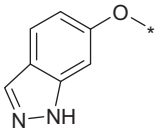	54	221	–
17	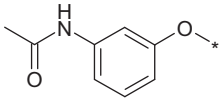	28	50	2290
18	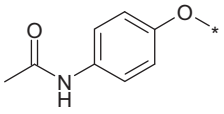	539	808	–
19	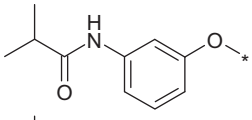	48	192	8810
20	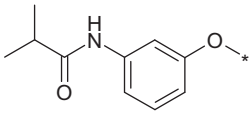	106	1310	
21	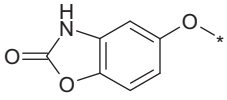	36	35	4510
22	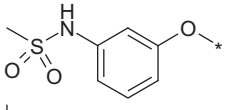	21	23	3800
23	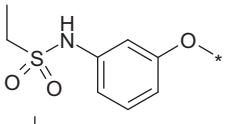	15	<30	**287**
24	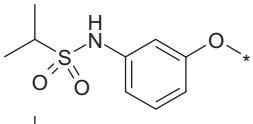	18	17	459
25	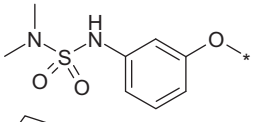	21	18	155
26	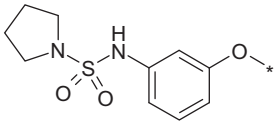	21	28	412

Table 3 (*continued*)

Compound	Side chain	In vitro IC_{50} (nM)		
		MEK1	A375 (B-Raf)	HCT116 (K-Ras)
27	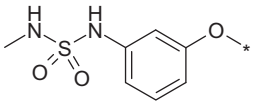	22	16	103
28	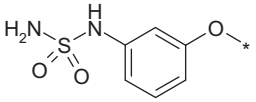	**14**	**4**	**180**
29	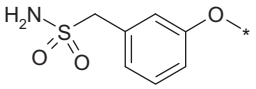	32	37	3490

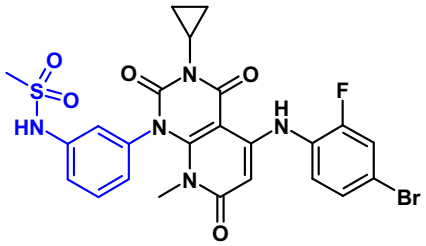

Figure 3. Structure of JTP-70902.

to better than 6 Å and were therefore not suitable for structure determination. The hydroxyl alkoxy side chain of **1** (Fig. 2) contacts the activation segment of MEK1 which in this crystal form contributes to a crystal contact with the corresponding activation loop of a crystal neighbor. Larger substituents in this area may thus have weakened this crystal contact which may have triggered the observed loss in diffraction power.

In conclusion, we have successfully established a novel series of allosteric MEK inhibitors by exploring previously unchartered SAR territories. We have identified sulfamide **28** as a highly potent

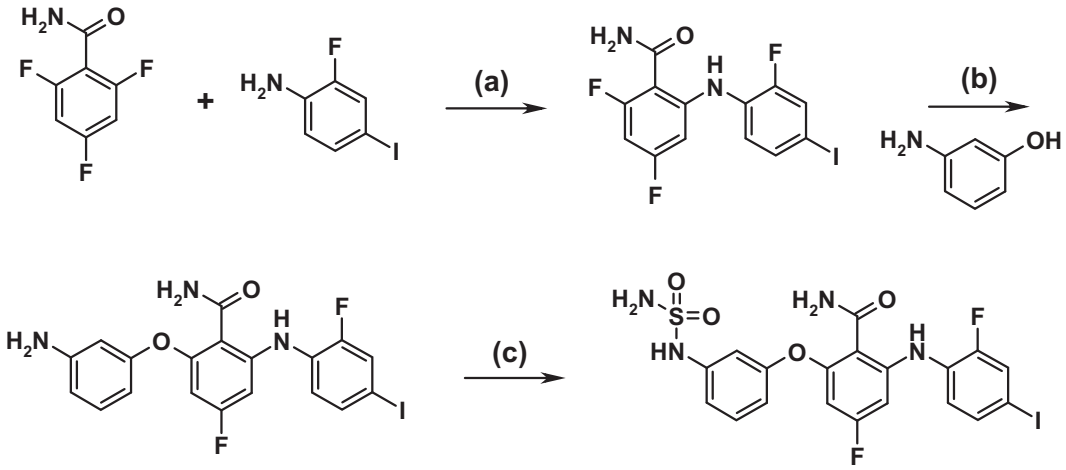

Scheme 1. Synthesis of sulfamide **28**. Reagents and conditions: (a) LiHMDS, THF, 0 °C to rt, 22%; (b) Cs_2CO_3, DMF, 50 °C, 73%; (c) (i) $ClSO_2NCO$, DMAc (cat.), CH_2Cl_2, HCO_2H, 40 °C, (ii) aniline intermediate, DIPEA, DMAc, rt, 82%. Abbreviations: DIPEA = diisopropylethylamine; DMAc = dimethylacetamide; LiHMDS = lithium hexamethyldisilazide.

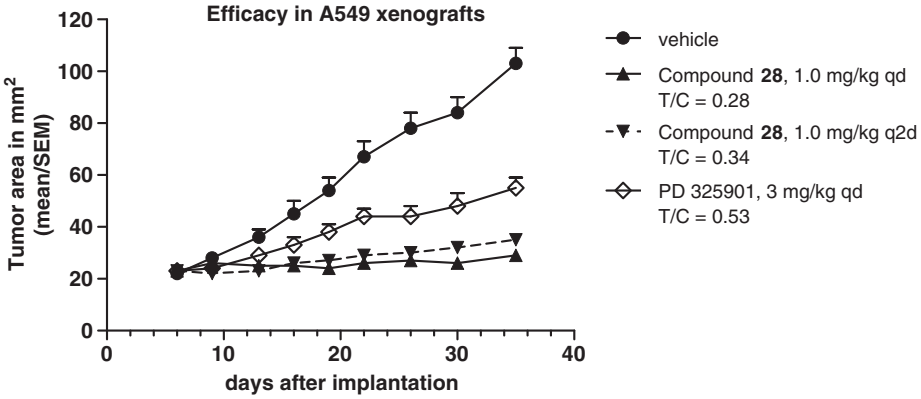

Figure 4. In vivo A549 xenograft study with sulfamide **28** and PD325901 in nude mice.

Table 4
PK data of key compounds

Compound	Rat PK[a]				Mice PK
	Cl_{blood} (L/kg/h)	V_{ss} (L/kg)	$t_{1/2}$ (h)	F (%)	Brain/plasma ratio[b]
PD325901	0.5	1.7	5.4	104	0.11
AZD6244	0.06	0.2	3.8	14–64	<0.02
1	1.49	4.4	2.4	70	0.73
8	0.58	10.3	8.4	20–41	0.04
28	0.03	2.0	32	62	<0.02

[a] Dosing for PD325901: 0.5 mg/kg iv/1 mg/kg po; dosing for AZD6244: 0.5 mg/kg iv/5 mg/kg po; dosing for **1**: 0.5 mg/kg iv/1 mg/kg po; dosing for **8**: 0.3 mg/kg iv/0.6 mg/kg po; dosing for **28**: 1 mg/kg iv/1 mg/kg po.
[b] AUC(brain)/AUC(plasma) for 0–3 h after 5 mg/kg iv dosing.

non-ATP competitive MEK inhibitor. With its ease of synthesis, its state-of-the-art in vivo efficacy in various xenograft models and its ability to continuously block ERK phosphorylation, sulfamide **28** was a significant milestone for our MEK inhibitor program. Further data on this compound and a subsequent round of optimization leading to a second generation of MEK inhibitors will be reported in due course.

Acknowledgments

We gratefully acknowledge Mario Lobell (Medicinal Chemistry Wuppertal, Bayer HealthCare AG) and our former colleagues at Bayer Pharmaceuticals West Haven Yingfu Li, Joachim Rudolph, Jacques Dumas, and Daniel Auclair for initiating this research project. We thank U. Hars, I. Korndoerfer and I. Moarefi at Crelux, Munich, for excellent service in protein purification, crystallization and crystal structure determination.

References and notes

1. (a) Roberts, P. J.; Der, C. *J. Oncogene* **2007**, *26*, 3291; (b) Montagut, C.; Settleman, J. *Cancer Lett.* **2009**, *283*, 125.
2. (a) Opar, A. *Nat. Rev. Drug Disc.* **2012**, *11*, 819; (b) Greger, J. G.; Eastman, S. D.; Zhang, V.; Bleam, M. R.; Hughes, A. M.; Smitheman, K. N.; Dickerson, S. H.; Laquerre, S. G.; Liu, L.; Gilmer, T. M. *Mol. Cancer Ther.* **2012**, *11*, 909; (c) Hatzivassiliou, G.; Liu, B.; O'Brien, C.; Spoerke, J. M.; Hoeflich, K. P.; Haverty, P. M.; Soriano, R.; Forrest, W. F.; Heldens, S.; Chen, H.; Toy, K.; Ha, C.; Zhou, W.; Song, K.; Friedman, L. S.; Amler, L. C.; Hampton, G. M.; Moffat, J.; Belvin, M.; Lackner, M. R. *Mol. Cancer Ther.* **2012**, *11*, 1143.
3. For an excellent compilation of allosteric MEK inhibitor patents until February 2008, see: Price, S. *Expert Opin. Ther. Patents* **2008**, *18*, 603.
4. More recent publications on novel allosteric MEK inhibitors in clinical development: (a) Iverson, C.; Larson, G.; Lai, C.; Yeh, L.-T.; Dadson, C.; Weingarten, P.; Appleby, T.; Vo, T.; Maderna, A.; Vernier, J.-M.; Hamatake, R.; Miner, J. N.; Quart, B. *Cancer Res.* **2009**, *69*, 6839; (b) Lee, L.; Niu, H.; Rueger, R.; Igawa, Y.; Deutsch, J.; Ishii, N.; Mu, S.; Sakamoto, Y.; Busse-Reid, R.; Gimmi, C.; Goelzer, P.; De Schepper, S.; Yoshimura, Y.; Barrett, J.; Ishikawa, Y.; Weissgerber, G.; Peck, R. *Clin. Cancer Res.* **2009**, *15*, 7368; (c) Kim, K.; Kong, S.-Y.; Fulciniti, M.; Li, X.; Song, W.; Nahar, S.; Burger, P.; Rumizen, M. J.; Podar, K.; Chauhan, D.; Hideshima, T.; Munshi, N. C.; Richardson, P.; Clark, A.; Ogden, J.; Goutopoulos, A.; Rastelli, L.; Anderson, K. C.; Tai, Y.-T. *Br. J. Haematol.* **2010**, *149*, 537; (d) Choo, E. F.; Belvin, M.; Chan, J.; Hoeflich, K.; Orr, C.; Robarge, K.; Yang, X.; Zak, M.; Boggs, J. *Xenobiotica* **2010**, *40*, 751; (e) Rice, K. D.; Aay, N.; Anand, N. K.; Blazey, C. M.; Bowles, O. J.; Bussenius, J.; Costanzo, S.; Curtis, J. K.; Defina, S. C.; Dubenko, L.; Engst, S.; Joshi, A. A.; Kennedy, A. R.; Kim, A. I.; Koltun, E. S.; Lougheed, J. C.; Manalo, J.-C. L.; Martini, J.-F.; Nuss, J. M.; Peto, C. J.; Tsang, T. H.; Yu, P.; Johnston, S. *ACS Med. Chem. Lett.* **2012**, *3*, 416; (f) Heald, R. A.; Jackson, P.; Savy, P.; Jones, M.; Gancia, E.; Burton, B.; Newman, R.; Boggs, J.; Chan, E.; Chan, J.; Choo, E.; Merchant, M.; Rudewicz, P.; Ultsch, M.; Wiesmann, C.; Yue, Q.; Belvin, M.; Price, S. *J. Med. Chem.* **2012**, *55*, 4594.
5. Haura, E. B.; Ricart, A. D.; Larson, T. G.; Stella, P. J.; Bazhenova, L.; Miller, V. A.; Cohen, R. B.; Eisenberg, P. D.; Selaru, P.; Wilner, K. D.; Gadgeel, S. M. *Clin. Cancer Res.* **2010**, *16*, 2450.
6. Adjei, A. A.; Cohen, R. B.; Franklin, W.; Morris, C.; Wilson, D.; Molina, J. R.; Hanson, L. J.; Gore, L.; Chow, L.; Leong, S.; Maloney, L.; Gordon, G.; Simmons, H.; Marlow, A.; Litwiler, K.; Brown, S.; Poch, G.; Kane, K.; Haney, J.; Eckardt, S. G. *J. Clin. Oncol.* **2008**, *26*, 2139.
7. In a recent publication, researchers of GSK described a similar reasoning: (a) Gilmartin, A. G.; Bleam, M. R.; Groy, A.; Moss, K. G.; Minthorn, E. A.; Kulkami, S. G.; Rominger, C. M.; Erskine, S.; Fisher, K. E.; Yang, J.; Zappacosta, F.; Annan, R.; Sutton, D.; Laquerre, S. G. *Clin. Cancer Res.* **2011**, *17*, 989; See also: (b) Abe, H.; Kikuchi, S.; Hayakawa, K.; Iida, T.; Nagahashi, N.; Maeda, K.; Sakamoto, J.; Matsumoto, N.; Miura, T.; Matsumura, K.; Seki, N.; Inaba, T.; Kawasaki, H.; Yamaguchi, T.; Kakefuda, R.; Nanayama, T.; Kurachi, H.; Hori, Y.; Yoshida, T.; Kakegawa, J.; Watanabe, Y.; Gilmartin, A. G.; Richter, M. C.; Moss, K. G.; Laquerre, S. G. *ACS Med. Chem. Lett.* **2011**, *2*, 320.
8. Ohren, J. F.; Chen, H.; Pavlovsky, A.; Whitehead, C.; Zhang, E.; Kuffa, P.; Yan, C.; McConnell, P.; Spessard, C.; Banotai, C.; Mueller, W. T.; Delaney, A.; Omer, C.; Sebolt-Leopold, J.; Dudley, D. T.; Leung, I. K.; Flamme, C.; Warmus, J.; Kaufman, M.; Barrett, S.; Tecle, H.; Hasemann, C. A. *Nat. Struct. Biol.* **2004**, *11*, 1192.
9. Barrett, S. D.; Bridges, A. J.; Dudley, D. T.; Saltiel, A. R.; Fergus, J. H.; Flamme, C. M.; Delaney, A. M.; Kaufman, M.; LePage, S.; Leopold, W. R.; Przybranowski, S. A.; Sebolt-Leopold, J.; Van Becelaere, K.; Doherty, A. M.; Kennedy, R. M.; Marston, D.; Howard, W. A., Jr.; Smith, Y.; Warmus, J. S.; Tecle, H. *Bioorg. Med. Chem. Lett.* **2008**, *18*, 6501.
10. After completion of our investigations, C5-substituted allosteric MEK inhibitors as well as more sterically demanding bicyclic cores have been reported: (a) Isshiki, Y.; Kohchi, Y.; Ikura, H.; Matsubara, Y.; Asoh, K.; Murata, T.; Kohchi, M.; Mizuguchi, E.; Tsujii, S.; Hattori, K.; Miura, T.; Yoshimura, Y.; Aida, S.; Miwa, M.; Saitoh, R.; Murao, N.; Okabe, H.; Beluni, C.; Janson, C.; Likacs, C.; Schück, V.; Shimma, N. *Bioorg. Med. Chem. Lett.* **2011**, *21*, 1795; (b) Laing, V. E.; Brookings, D. C.; Carbery, R. J.; Simorte, J. G.; Hutchings, M. C.; Langham, B. J.; Lowe, M. A.; Allen, R. A.; Fetterman, J. R.; Turner, J.; Meier, C.; Kennedy, J.; Merriman, M. *Bioorg. Med. Chem. Lett.* **2012**, *22*, 472; (c) Adams, M. E.; Wallace, M. B.; Kanouni, T.; Scorah, N.; O'Connell, S. M.; Miyake, H.; Shi, L.; Halkowycz, P.; Zhang, L.; Dong, Q. *Bioorg. Med. Chem. Lett.* **2012**, *22*, 2411.
11. Tecle, H. *Presented at the Residential School on Medicinal Chemistry*; Drew University: NJ/USA, June, 2006.
12. Rudolph, J.; Dumas, J.; Li, Y.; Auclair, D.; Lobell, M Unpublished results Bayer HealthCare AG 2006-7. For a related study, see: Tecle, H.; Shao, J.; Li, Y.; Kothe, M.; Kazmirski, S.; Penzotti, J.; Ding, Y.-H.; Ohren, J.; Moshinsky, D.; Coli, R.; Jhawar, N.; Bora, E.; Jacques-O'Hagan, S.; Wu, J. *Bioorg. Med. Chem. Lett.* **2009**, *19*, 226.
13. (a) For detailed assay descriptions, further synthetic details and analytical data of example compounds, see: Rudolph, J.; Dumas, J.; Li, Y.; Auclair, D.; Lobell, M.; Hitchcock, M.; Hartung, I.; Koppitz, M.; Brittain, D.; Puehler, F.; Petersen, K.; Guenther, J. PCT Patent WO 2008/138639.; (b) Hitchcock, M.; Hartung, I. PCT Patent WO 2009/129938.
14. Cell proliferation inhibition data were correlated in selected cases to measurements of pERK inhibition in the respective cell lines (Mesoscale assay set-up) to rule out off-target cytotoxicity. As pERK inhibition IC_{50} values in general paralleled proliferation IC_{50} values the former are—for the sake of clarity—excluded from this manuscript.
15. Solit, D. B.; Garraway, L. A.; Pratilas, C. A.; Sawai, A.; Getz, G.; Basso, A.; Ye, Q.; Lobo, J. M.; She, Y.; Osman, I.; Golub, T. R.; Sebolt-Leopold, J.; Sellers, W. R.; Rosen, N. *Nature* **2006**, *439*, 358.
16. (a) Yamaguchi, T.; Yoshida, T.; Kurachi, R.; Kakegawa, J.; Hori, Y.; Nanayama, T.; Hayakawa, K.; Abe, H.; Takagi, K.; Matsuzaki, Y.; Koyama, M.; Yogosawa, S.; Sowa, Y.; Yamori, T.; Tajima, N.; Sakai, T. *Cancer Sci.* **1809**, *2007*, 98; A close analog of JTP-70902 was later-on advanced to clinical development under the name GSK 1120212: see Ref. 7. For a more recently reported related series from Takeda, see: (b) Dong, Q.; Dougan, D. R.; Gong, X.; Halkowycz, P.; Jin, B.; Kanouni, T.; O'Connell, S. M.; Scorah, N.; Shi, L.; Wallace, M. B.; Zhou, F. *Bioorg. Med. Chem. Lett.* **2011**, *21*, 1315.
17. (a) Bagal, S. K.; Bungay, P. J. *ACS Med. Chem. Lett.* **2012**, *3*, 948; (b) Di, L.; Rong, H.; Feng, B. *J. Med. Chem.* **2013**, *56*, 2.